Proceedings of the
44th IEEE Conference on Decision and Control, and
the European Control Conference 2005
Seville, Spain, December 12-15, 2005

Robust lateral controller for 4-wheel steer cars with actuator constraints

D.J.Leith, W.E.Leithead and M.Vilaplana
Hamilton Institute, National University of Ireland, Maynooth, Ireland.

Abstract— **In this paper we study a new steering controller for cars equipped with 4-wheel steer-by-wire. The controller commands front and rear steering angles with the objective of tracking reference yaw rate and sideslip signals corresponding to the desired vehicle handling behaviour. The controller compensates for changes in vehicle dynamics with forward speed and incorporates an anti-windup scheme to mitigate the effects of the saturation or failure of the rear steering actuators. We analyse the robust stability and performance of the resulting non-linear control system.**

I. Introduction

The concept of generic prototype vehicles has emerged as a promising solution to an outstanding challenge in the development of ride and handling characteristics for advanced passenger cars: the bridging of the gap between numerical simulations based on a vehicle model—a virtual prototype—and experiments on a proof-of-concept prototype vehicle. A generic prototype vehicle would be equipped with advanced computer-controlled actuators enabling it to modify its ride and handling characteristics. Examples of such advanced actuators are four and rear steer-by-wire, brake-by-wire and active suspensions. An integrated chassis controller would command those actuators to track a set of reference signals corresponding to a desired ride and handling behaviour. Currently, moving-base driving simulators are used to emulate the ride and handling behaviour of virtual prototypes prior to building real ones. However, the achievable accelerations of such simulators severely constrain their ability to realistically recreate the full range of vehicle motion. Generic prototype vehicles could allow for the realistic recreation of the ride and handling characteristics of virtual prototypes, thereby enabling engineers to experience and evaluate their behaviour prior to making the decision of building expensive proof-of-concept prototypes.

In this paper, we present a steering controller that enables cars equipped with 4-wheel steer-by-wire to display predefined handling characteristics. This steering controller is intended as a first step towards an integrated chassis controller for a generic prototype vehicle. The proposed steering controller commands front and rear steering angles with the objective of tracking reference yaw rate and sideslip angle signals obtained online from the driver's inputs to steering wheel and pedals. These reference signals describe the lateral dynamic response to those inputs of a virtual prototype with the desired handling characteristics. The steering controller automatically rejects disturbances in sideslip and yaw rate, such as those caused by μ-split braking manoeuvres or lateral wind gusts. In addition, we deal with the issue, often overlooked in the literature, of ensuring that the steering controller remains robustly stable and performs satisfactorily in the event of rear steering actuator saturation.

A substantial body of research on the control of 4-wheel steering cars already exists and a variety of control structures have been proposed in the literature. Most of these structures rely on the use of gain-scheduled feedforward control to command the rear steering angle [1]. An example of an steering controller specifically designed for cars equipped with 4-wheel steer-by-wire is presented in [2].

Since the steering controller considered here is intended as the foundation for an integrated chassis controller, the main design criteria are transparency, simplicity and modularity. The structure of the steering controller presented in this paper is based on a physical model of the lateral dynamics of 4-wheel steering cars. The main elements of the controller structure are a linear input transformation and a speed-dependent inner feedback loop. This structure partially decouples the sideslip and yaw rate responses to the new controllable inputs, with the yaw rate response being speed-invariant. Thus, the proposed structure acts as an implicit gain scheduling on the vehicle speed. The resulting 2-by-2 multivariable control design problem is restated as two single-input, single-output (SISO) control design problems according to the ICD paradigm. Assuming certain bandwidth restrictions, individual linear controllers for the resulting sideslip and yaw rate channels can be designed using classical techniques.

II. Simplified vehicle model

For small values of front and rear wheel slip angles α_f and α_r, and disregarding the dynamics of the tyre force generation, the forces S_f and S_r (see Figure 1) can be approximated by the following expressions: [3]:

$$S_f = K_f \alpha_f \quad (1)$$

$$S_r = K_r \alpha_r \quad (2)$$

The constant K_f is the result of modifying the combined stiffness of the two front tyres to take into account the caster effect of the steering system at the front axle. Since no caster effect is generated at the rear axle, the constant K_r is simply the cornering stiffness. This yields the following state-space representation with the two steering angle inputs (δ_f and δ_r) and side-slip angle β and yaw rate $\dot{\psi}$ as outputs,

$$\dot{x} = A(v)x + B(v)u \quad (3)$$

$$y = Cx \quad (4)$$

0-7803-9568-9/05/$20.00 ©2005 IEEE

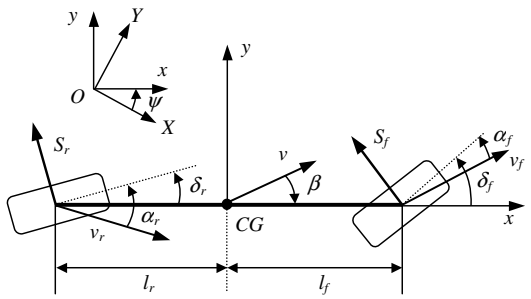

Fig. 1. Single-track model of a 4-wheel steering car

where v is the vehicle forward speed,

$$u = \begin{bmatrix} \delta_f \\ \delta_r \end{bmatrix}, \quad y = x = \begin{bmatrix} \beta \\ \dot{\psi} \end{bmatrix} \tag{5}$$

$$A(v) = \begin{bmatrix} -\dfrac{K_f + K_r}{mv} & \dfrac{K_f l_f - K_r l_r}{mv^2} + 1 \\ \dfrac{K_f l_f - K_r l_r}{I_{zz}} & -\dfrac{K_f l_f^2 + K_r l_r^2}{I_{zz} v} \end{bmatrix} \tag{6}$$

$$B(v) = \begin{bmatrix} -\dfrac{K_f}{mv} & -\dfrac{K_r}{mv} \\ \dfrac{K_f l_f}{I_{zz}} & -\dfrac{K_r l_r}{I_{zz}} \end{bmatrix}, C = \begin{bmatrix} 1 & 0 \\ 0 & 1 \end{bmatrix} \tag{7}$$

We note that although the dynamics are speed dependent, the longitudinal inertia of the vehicle is much larger than the the rotational inertia about the vertical axis. Hence, changes in longitudinal speed inherently occur on a longer time scale than changes in the lateral variables yaw rate and sideslip; that is, we can assume that the speed is slowly varying.

III. Steering controller

A. Input transformation

Using the linear input transformation

$$\begin{bmatrix} \delta_f \\ \delta_r \end{bmatrix} = E \begin{bmatrix} \Delta_1 \\ \Delta_2 \end{bmatrix} \tag{8}$$

where

$$E = -\frac{1}{\frac{K_r}{K_f}\left(1 + \frac{l_r}{l_f}\right)} \begin{bmatrix} \dfrac{K_r l_r}{K_f l_f} & -\dfrac{K_r}{K_f} \\ -1 & -1 \end{bmatrix} \tag{9}$$

the transformed plant input matrix $B(v)E$ is made diagonal with

$$B(v)E = \begin{bmatrix} -\dfrac{K_f}{mv} & 0 \\ 0 & \dfrac{K_f K_f}{I_{zz}} \end{bmatrix} \tag{10}$$

A physical interpretation of the new inputs is in terms of a mode given by Δ_1, which excites the sideslip by steering front and rear wheels in the same direction, and a mode given by Δ_2, which excites the yaw rate by steering front and rear wheels in opposite directions.

B. Speed-dependent feedback

We next introduce a feedback element of the form $\Delta = \tilde{\Delta} - F(v)y$ which results in the new vector of controllable inputs $\tilde{\Delta} = \begin{bmatrix} \tilde{\Delta}_1 \\ \tilde{\Delta}_2 \end{bmatrix}$. Let the matrix $F \in \mathbb{R}^{2\times 2}$ be

$$F = \begin{bmatrix} 0 & 0 \\ K_2 & K_v(v) \end{bmatrix} \tag{11}$$

with $K_v(v) = K_0 - \frac{\lambda}{K_1}$, $K_0 = \frac{K_f l_f^2 + K_r l_r^2}{K_f l_f v_0}$, $K_1 = \frac{K_f l_f}{I_{zz}}$ and $K_2 = 1 - \frac{K_r l_r}{K_f l_f}$ where v_0 is an arbitrary fixed vehicle speed and λ is a constant. We then have that

$$\dot{x} = A(v)x + B(v)E(\tilde{\Delta} - F(v)x) \tag{12}$$

$$= (A(v) - B(v)EF(v))x + B(v)E\tilde{\Delta} \tag{13}$$

where $A(v) - B(v)EF(v)$ is upper triangular and $B(v)E$ diagonal. The resulting yaw rate dynamics

$$\ddot{\psi} = -\lambda\dot{\psi} + K_1\tilde{\Delta}_2 \tag{14}$$

are now invariant with vehicle speed, v, and depend only on the input $\tilde{\Delta}_2$.

Figure 2 shows the Bode plots of the elements of the resulting transfer function $\tilde{G}(s)$ for different vehicle speeds. In the figure observe that $\tilde{G}(s)$ is only approximately upper-triangular as this plot includes additional plant dynamics—time delay, actuators, tyre force and caster dynamics—that are not present in the simplified model above. In Figure 2 it can also be seen that with this more complete representation the yaw rate dynamics are not completely speed-invariant but they can be considered so up to a frequency of around 10 rad/s. Similarly, the sideslip dynamics are not speed-invariant but they can be considered so up to a frequency of around 2 rad/s.

C. Diagonal controller

Using the above input transformation and speed-dependent feedback, a diagonal controller now suffices, see Figure 3. Simple linear controllers

$$\tilde{k}_1(s) = -\frac{K_{1I}}{s}, \quad \text{I Controller} \tag{15}$$

$$\tilde{k}_2(s) = K_{2p} + \frac{K_{2I}}{s}, \quad \text{PI controller} \tag{16}$$

$$\tag{17}$$

can easily be tuned to obtain satisfactory performance with a low bandwidth sideslip channel (approx 2 rad/s) and a high bandwidth yaw rate channel (approx 10 rad/s). The speed-dependent feedback term $K_v(v_x)$ acts as an implicit gain scheduling scheme that combines linear controllers parameterised by the vehicle speed into a non-linear controller valid for varying speed.

D. Anti-windup

The steering controller has been designed without considering the possible saturation of the rear steering actuators. While the maximum allowable front rear steering angle ($\pm 40^0$) is not likely to be reached in the driving situations in

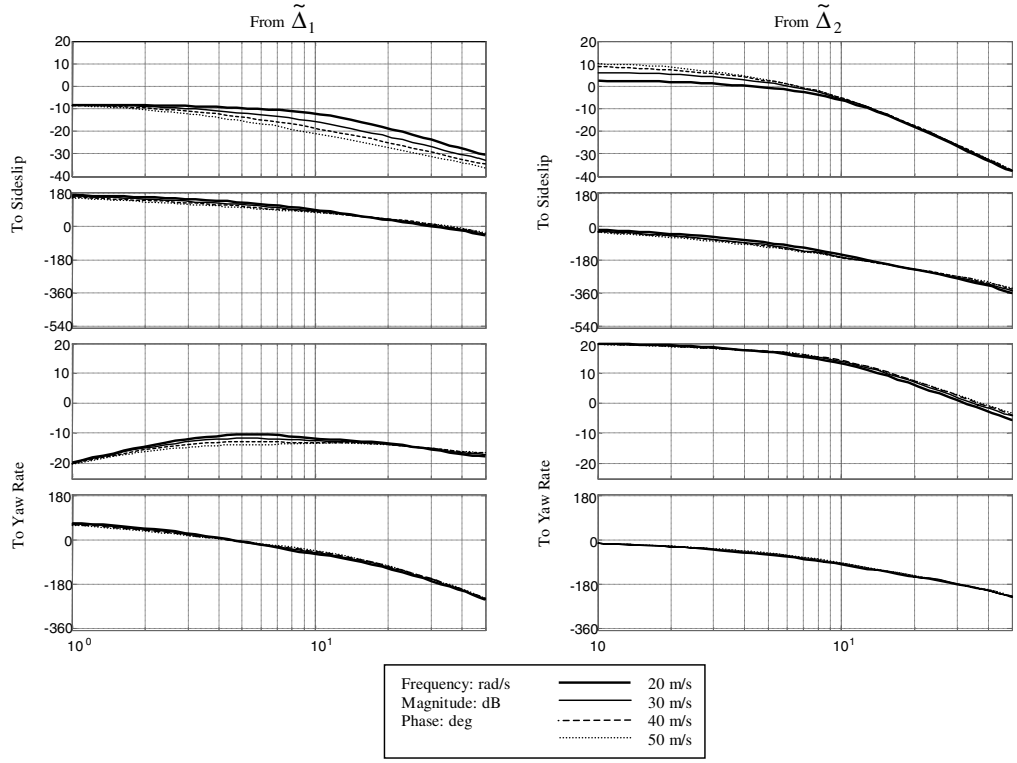

Fig. 2. Bode plot of $\tilde{G}(s)$ for different vehicle speeds

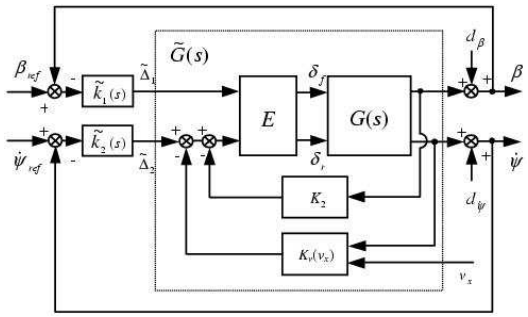

Fig. 3. Transformed multivariable control design problem

which the controller will operate, the possible saturation of the rear actuators has to be considered since the maximum allowable rear steering angle is restricted to only $\pm 5^0$ due to space constraints. The nonlinearity introduced by saturating rear actuators can cause a significant performance degradation with respect to the nominal linear operation of the system. In extreme circumstances, saturation may even lead to instability. The proposed anti-windup scheme is inspired by conventional anti-windup methods for SISO systems and works as follows. The rear steering angle signal commanded by the controller is subtracted from the actual rear steering angle. The resulting signal is fed to the input of the controller $\tilde{k}_1(s)$ through a gain K_{AW}. The performance of this scheme is illustrated in Figure 4. This shows results where the car travels on a road with a μ-split surface so that the two wheels at the left hand side of the car are on dry asphalt (friction coefficient, $\mu \approx 1$) and the two on the right hand side are on ice (friction coefficient $\mu \approx 0.2$). While turning at 50 m/s, the driver applies the brakes moderately for 1 s without moving the steering wheel. The simulation results illustrate the response of the controlled car with and without anti-windup. As it can be seen in the figure, the driver applies the brakes between time = 8 s and time = 9 s. The steering controller attempts to automatically reject the disturbances introduced during braking while tracking the reference sideslip and yaw rate signals. This results in the saturation of the rear actuators. Without anti-windup, the controller is not able to recover from the disturbances and spins out of control. On the other hand, the full steering controller (with anti-windup) is able to retain control of the car.

IV. Robust stability analysis

A. Parametric uncertainty

We study the robustness of the controlled system against structured (parametric) uncertainty and adopt a frequency domain representation of the parametric uncertainty in the plant elements. At any given frequency, we consider neighborhoods of structured uncertainty around the points in the complex plane corresponding to the values of the nominal transfer functions g_{ij}^{nom}. The neighborhood of structured uncertainty around a transfer function element at a given frequency encloses all the values that the transfer function may take considering all possible values of the uncertain

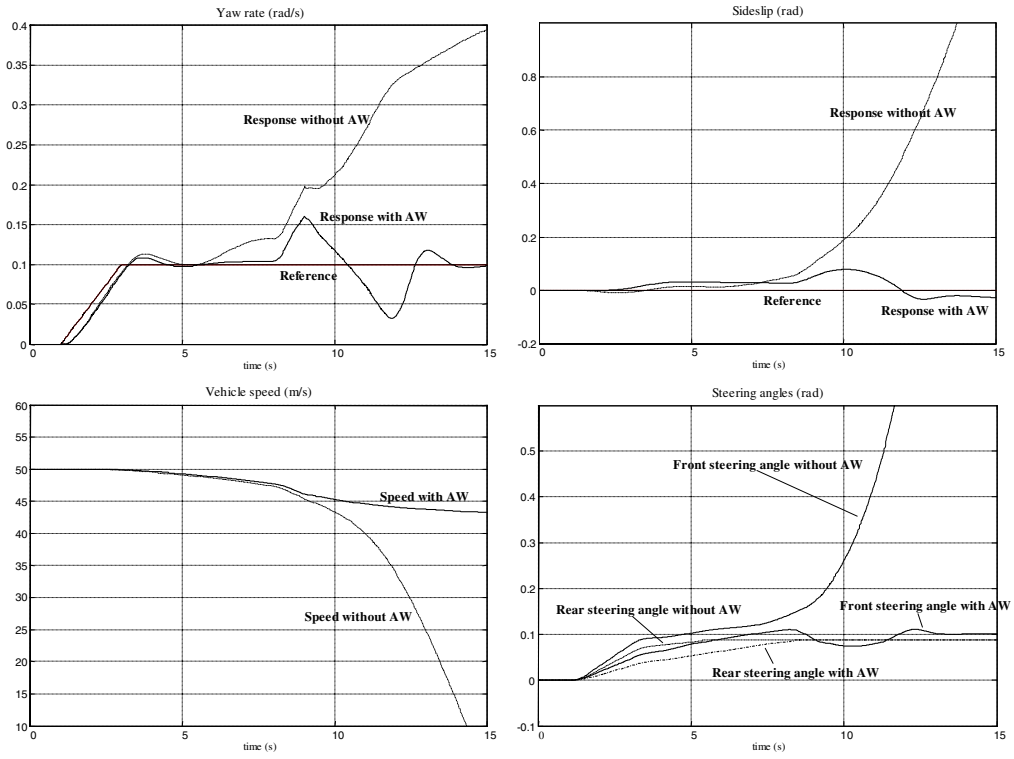

Fig. 4. Performance of the controller when the rear actuators saturate

TABLE I

RANGES OF VARIATION OF THE MODEL PARAMETERS.

Parameter	Variation about nominal value
Mass, m	$\pm 12\%$
Inertia, I_{zz}	$\pm 12\%$
Tyre stiffness, C_T	$+10\% - 30\%$
Steering elasticity, C_L	$\pm 10\%$
Caster, n_s	$\pm 15\%$
Tyre force dynamics, a	$\pm 10\%$

parameters in the plant model. We define the structured uncertainty for $g_{ij}(j\omega)$ as:

$$\Delta^s g_{ij}(j\omega) = g_{ij}(j\omega) - g_{ij}^{nom}(j\omega) \tag{18}$$

where $g_{ij}(j\omega)$ is the value of the transfer function for any given set of allowable model parameters. The neighborhoods of structured uncertainty may be irregularly shaped. The function $\Delta^s g_{ij}(j\omega)$ defines the neighborhood of structured uncertainty around $g_{ij}^{nom}(j\omega)$ at the frequency ω.

To generate the neighborhoods of structured uncertainty, we sample the intervals of possible values of each of the uncertain parameters according to a uniform distribution. Table IV-A shows typical ranges of variation used to generate the intervals from which to sample. Note that the tyre stiffness C_T is allowed to take values of up to 30% below its nominal one. Such a large range of variation caters for the reductions in the tyre stiffness occurring when the road surface is wet or icy.

Figure 5 shows the nominal Nyquist plot of the transmittance of the sideslip channel together with the neighborhoods of parametric uncertainty at several frequencies ranging from 1 rad/s to 20 rad/s. It can be seen that the parametric uncertainty generally tends to increase with the vehicle speed and to decrease with frequency.

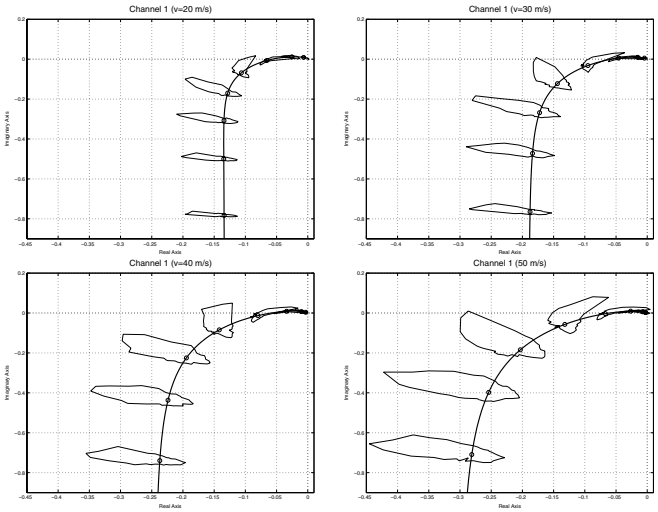

Fig. 5. Nyquist plots of sideslip channel and neighborhoods of structured uncertainty for different vehicle speeds.

Figure 6 shows the nominal Nyquist plot of the transmittance of the yaw rate, together with the neighborhoods of parametric uncertainty at several frequencies ranging from 1 rad/s to 20 rad/s. Again, it can be seen that impact of the

parametric uncertainty increases with the vehicle speed and decreases with frequency.

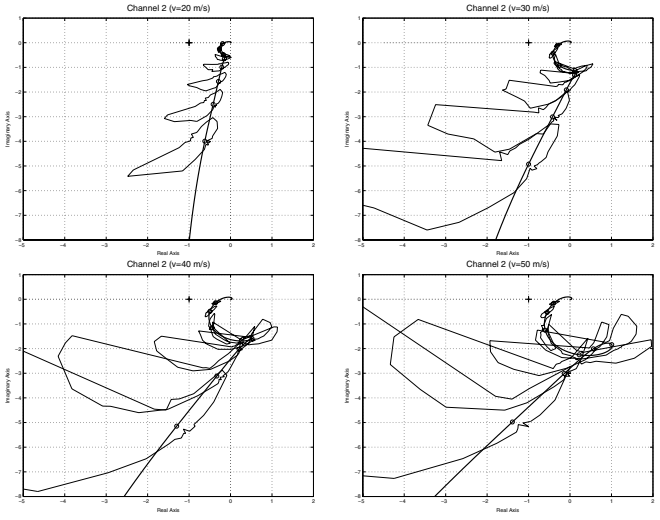

Fig. 6. Nyquist plots of yaw rate channel and neighborhoods of structured uncertainty for different vehicle speeds.

B. Stability of constrained system

In this subsection, we analyse the robust stability of the control system considering the possible saturation of the rear steering actuators. To study the stability of the system, we transform it into an equivalent one whose forward path contains a SISO linear time-invariant subsystem and whose feedback path contains the saturation nonlinearity. The equivalent system, which is depicted in Figure 7, is an example of a Lur'e system. Thus, asymptotic stability results developed for Lur'e systems, such as the Circle Criterion ([4],[5]), can be used in the analysis.

The closed-loop system now takes the form

$$\dot{x} = (A^l - k_{nl}(\delta_{r,c}))x \tag{19}$$

$$\tag{20}$$

where $\delta_{r,c}$ is the rear steering angle demanded by the controller. The nonlinear function k_{nl} represents the saturation nonlinearity and is given by

$$k_{sat}(\delta_{r,c}) = \begin{cases} 1 & \text{if } |\delta_{r,c}| \leq \delta_{sat} \\ \dfrac{\delta_{max}}{|\delta_{r,c}|} & \text{if } |\delta_{r,c}| > \delta_{sat} \end{cases} \tag{21}$$

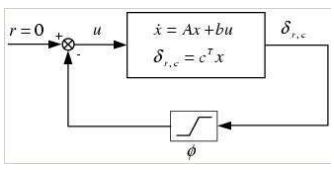

Fig. 7. Equivalent control system for stability analysis: a Lur'e problem

Here δ_{sat} is the absolute value of the steering angles at which the rear actuators saturate. Note that the function $k_{sat}(\delta_{r,c})$ can be written as a function of the state and $0 \leq k_{sat}(x) \leq 1$ for all x. Now, if there is a positive definite matrix P such that

$$(A^l)^T P + P A^l < 0, \quad (A^l - bc^T)^T P + P(A^l - bc^T) < 0 \tag{22}$$

then $V(x^l) = (x^l)^T P x^l$ will define a Lyapunov function for the system (19), thus assuring its asymptotic stability. This follows because all of the matrices that arise in (19) are convex combinations of the two matrices $A^l, A^l - bc^T$. Thus if there is a solution P to (22), this guarantees the asymptotic stability of (19).

The Circle Criterion provides a frequency domain condition that can be used to test for the existence of a solution to (22). It has recently been shown that it is also possible to test for the existence of such a solution using a simple time-domain condition ([6],[7]). Specifically, there is a positive definite P satisfying (22) if and only if the matrices A^l and $(A^l - bc^T)$ are Hurwitz, i.e. their eigenvalues lie in the open left half of the complex plane, and their product $A^l(A^l - bc^T)$ has no negative real eigenvalues. We use this fact to analyse the robust stability of our control system with respect to parametric uncertainty. A major advantage of the time-domain condition is its simplicity, as it only requires the calculation of one set of eigenvalues as opposed to checking a frequency domain condition for infinitely many values of a variable.

Figure 8 summarises the results of the analysis. Figure 8 wass obtained as follows. First the steering controller was tuned for the nominal values of the car model parameters. The real values of those parameters are uncertain, each of them lying within an interval around its nominal value. For a given fixed vehicle speed, we calculated the entries of A^l, b and c for a large number (1000) of sets of parameter values randomly chosen from their respective uncertainty intervals—the ranges of parameter variations are those given in Table IV-A above. We checked that for all those sets of parameter values, the matrices A^l and $(A^l - bc^T)$ remained Hurwitz. We then calculated the eigenvalues of $A^l(A^l - bc^T)$ for all the sets of parameter values considered. We repeated the process outlined above for three different vehicle speeds: 20 m/s, 35 m/s and 50 m/s. For each of the three speeds considered, we have plotted the eigenvalues closest to the real negative axis obtained with the different sets of random parameter values. As it can be seen in the figure, the eigenvalues of the matrix product $A^l(A^l - bc^T)$ remain well clear of the real negative axis. In light of the above, we conclude that the control system in Figure 7 is robustly asymptotically stable for the speeds considered. We can then affirm that our original control system is robustly BIBO stable for those speeds.

To illustrate how the value of the anti-windup gain K_{AW} may affect the stability of the system we have generated a figure similar to Figure 8 with a value of K_{AW} smaller than

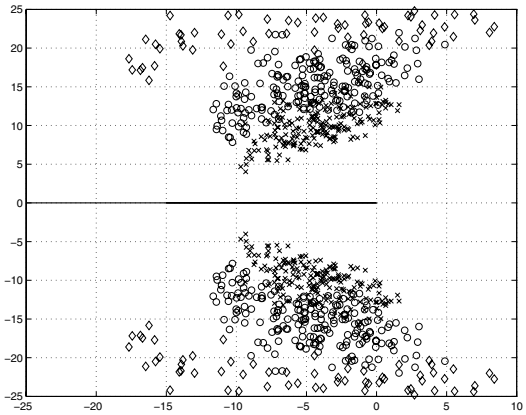

Fig. 8. Closest eigenvalues to the real negative axis for random parameter values and different vehicle speeds: ◇: 20 m/s; ○: 35 m/s; ×: 50 m/s.

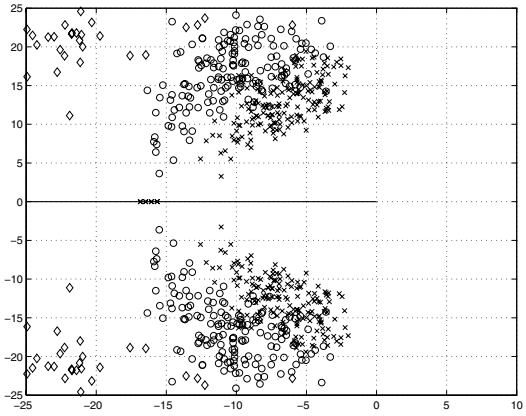

Fig. 9. Closest eigenvalues to the real negative axis for random parameter values and different vehicle speeds with a smaller value of K_{AW}: ◇: 20 m/s; ○: 35 m/s; ×: 50 m/s.

the one selected for the controller through the tuning process. In the resulting plot, shown in Figure 9, we observe that the eigenvalues of $A^l(A^l - bc^T)$ are generally closer to the negative real axis than in Figure 8 and, in fact, $A^l(A^l - bc^T)$ actually has real negative eigenvalues at 50 m/s for some sets of allowable parameter values. Consequently, we can state that, for that speed, there is no positive definite solution P to (22) and we can neither confirm or refute the asymptotic stability of the system—it may or may not be stable at that speed. Thus, this choice of K_{AW} prevents us from reaching any conclusions about the stability of the system using the proposed approach.

V. Experimental results

The controller has been implemented on a Mercedes S Class equipped with 4-wheel steer-by-wire. Typical results from the test drives are shown in Figure 10. The reference signals described the response of a sporty car to the driver's inputs. The experimental results confirm the robustness of the controller and illustrate its ability to artificially modify the handling behaviour of the vehicle with varying speed.

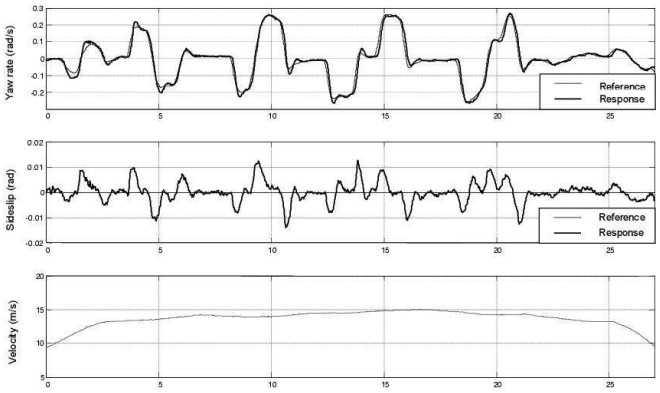

Fig. 10. Experimental results.

VI. Conclusions

In this paper, we have presented a new steering controller for cars equipped with 4-wheel steer-by-wire. The controller allows the car to track given reference sideslip and yaw rate signals while rejecting external disturbances. Schematically, the controller comprises four distinct functional elements: a linear input transformation and a feedback element scheduled with the vehicle speed, which together render the yaw rate dynamics nearly speed-invariant with respect to the new controllable inputs; a linear diagonal controller valid for all operating vehicle speeds, which provides robustness and disturbance rejection performance; an anti-windup scheme, which allows the controller to perform satisfactorily when the rear actuators saturate. We have analysed the robust stability of the control system using recent results from the theory of common quadratic Lyapunov functions. The performance and robustness of the control system have been demonstrated through simulation and experimental testing on a test car equipped with 4-wheel steer-by-wire.

VII. Acknowledgements

This work was supported by EU STREP grant CEMACS.

References

[1] Furukawa, Y., Yuhara, N., Sano, S., Takeda, H., Matsushita, Y.: A review of four-wheel steering studies from the viewpoint of vehicle dynamics and control. Vehicle System Dynamics **18** (1989) 151–186

[2] Ackermann, J.: Robust decoupling, ideal steering dynamics and yaw stabilization of 4WS cars. Automatica **30** (1994) 1761–1768

[3] Guillespie, T.D.: Fundamentals of vehicle dynamics. Society of Automotive Engineers (1992)

[4] Narendra, K. S., Goldwyn, R. : A geometrical criterion for the stability of certain nin-linear, non-autonomous systems. IEEE Transactions on Circuit Theory **11** (1964) 406–407

[5] Willems, J.: The circle criterion and quadratic Lyapunov functions for stability analysis. IEEE Transactions on Automatic Control **18** (1973) 184

[6] Shorten, R. N., Narendra, K. S.: On common quadratic Lyapunov functions for pairs of stable LTI systems whose system matrices are in companion form. IEEE Transactions on Automatic Control **48** (2003) 618–621

[7] Shorten, R. N., Mason, O., O'Cairbre, F., Curran, P.: A unifying framework for the SISO circle criterion and other quadratic stability criteria. International Journal of Control **77** (2004) 1–8